Asian Journal of Research and Reviews in Physics

4(3): 42-65, 2021; Article no.AJR2P.70740
ISSN: 2582-5992

Impacts of the Variations of Aerosols Components and Relative Humidity on the Visibility and Particles Size Distribution of the Desert Atmosphere

S. U. Yerima[1*], B. I. Tijjani[2] and U. M. Gana[2]

[1]Nigerian Meteorological Agency (NIMET), Nnamdi Azikwe International Airport Abuja, Nigeria.
[2]Department of Physics, Bayero University Kano, Kano State, Nigeria.

Authors' contributions

This work was carried out in collaboration among all authors. All authors read and approved the final manuscript.

Article Information

DOI: 10.9734/AJR2P/2021/v4i330146
Editor(s):
(1) Prof. Shi-Hai Dong, National Polytechnic Institute, Mexico.
Reviewers:
(1) Aleixandre Herrero, Japan.
(2) Davidson Odafe Akpootu, Usmanu Danfodiyo University Sokoto, Nigeria.
Complete Peer review History: https://www.sdiarticle4.com/review-history/70740

Original Research Article

Received 07 May 2021
Accepted 23 July 2021
Published 28 July 2021

ABSTRACT

This paper investigates the Impact of relative humidity, varying the concentrations of water-soluble aerosol particle concentrations (WASO), Mineral Nuclei Mode Aerosols Particle Concentration (MINN), mineral accumulation mode, nonspherical (MIAN) aerosol particles concentrations and Mineral Coarse Mode Aerosols Particle Concentration (MICN) on the visibility and particles size distribution of desert aerosols based on microphysical properties of desert aerosols. The microphysical properties (the extinction coefficients, volume mix ratios, dry mode radii and wet mode radii) were extracted from Optical Properties of Aerosols and Clouds (OPAC 4.0) at eight relative humidities, RHs (00 to 99%) and at the spectral visible range of 0.4-0.8μm, the concentrations were varied to obtain five different models for each above-mentioned component. Regression analysis of some standard equations were used to determine the Angstrom exponent (α), the turbidity coefficient (β), the curvature (α_2), humidification factor (γ), the mean exponent of aerosol growth curve (μ) and the mean exponent of aerosol size distributions (μ). The values of angstrom exponent (α) were observed to be less than 1 throughout the five models at all RHs for the four studied components, and this signifies the dominance of coarse mode particles over fine mode particles. But the magnitude of the angstrom exponent (α) fluctuates all through the studied

**Corresponding author: E-mail: sunusiyerima@yahoo.com, sunusiyerima86@gmail.com;*

components except for WASO which increased with the increase in RH across the models and this also signifies the dominance of coarse mode particles with some traces of fine mode particles. The investigation also revealed that the curvature (α_2) has both monomodal (negative signs) and bimodal (positive signs) types of distributions all through the five models and this also signifies the dominance of coarse mode particles with some traces of fine mode particles across the individual models for all the studied components. it was also found that the visibility decreased with the increase in RH and increased with the increase in wavelength. The investigation further revealed that the turbidity coefficient (β) fluctuates with the increase in RH and the particles concentrations, and this might be due to major coagulation and sedimentation. The analysis further found that there is a direct inverse power relation between the humidification factor and the mean exponent of aerosols size distribution with the mean exponent of aerosols growth curve. It was also found that as the magnitude of μ increased for MIAN, MINN and MICN, the effective hygroscopic growth g_{eff} decreased. For WASO, it was found that as the magnitude of μ decreased, the effective hygroscopic growth g_{eff} increased with the increase in particles concentrations and RH. The decreased in the magnitude of μ for WASO might be due to the fact that as we increase the non-hygroscopic particles, we decrease the deliquescence. The mean exponent of aerosol size distribution (μ) being less than 3 shows foggy condition of the desert atmosphere the four investigated components and five studied models.

Keywords: Extinction coefficient; visibility enhancement parameter; mean exponent of the aerosol size distribution; humidification factor; mean exponent of the aerosol growth curve.

1. INTRODUCTION

The Atmospheric interactions of aerosols with environments are complex because of the types of their sources, evolution, and interactions with water vapor in the atmosphere. They influence the climate directly by absorbing as well as reflecting the incoming short-wave solar radiation back to space [1]. Aerosols change the Earth's climate directly by scattering or absorbing solar radiation and indirectly by modifying the cloud characteristics [2]. Hygroscopicity (i.e., water vapor affinity) of atmospheric aerosol particles is also one of the key factors in defining their impacts on the atmosphere. These aerosol particles revealed changes in their microphysical and optical properties with relative humidity (RH) due to the water uptake. These changes depend on the particles' chemical composition, size and the ambient relative humidity (RH) [3–5]. Depending on the chemical compositions, aerosol particles can take up large amounts of water compared to their dry state as relative humidity (RH) increases and this can radically increase their sizes cause changes in the effective indices, effective radii and their optical properties [5-6].

Desert aerosols are known to change the climate transformation but they still constitute one of the largest uncertainties in climate change studies [7]. Mineral dust is mainly obtained from Desert which spread across the desert atmosphere [8]. There particles have serious effect on both regional and global climate through their interaction with solar and terrestrial radiation [9]. Desert aerosols particles exhibit hygroscopic growth due to chemical transformations and water uptake which occurred during long-range transport [7].

In the natural environments the changes in the microphysical and optical properties observed at a given wavelength are signs that measuring conditions have changed. These changes can cause unbalance in the atmosphere by causing decrease in visibility or other harmful effects to man and his environment, it might also be related either to an increase in RH or to a change in the aerosol concentration. These detailed changes are not always available for ambient aerosol [10]. Moreover, the impacts of relative humidity and varying the concentrations of the four components of dessert aerosols on the visibility of the desert atmosphere can cause harmful effects on human health, visibility degradation, and can also affect signal propagation in communication industry. Hence the need to properly study the effect of varying the concentration and water uptake of the mineral transported nuclei aerosols on visibility of the desert atmosphere. The properties of aerosols and clouds are very inconsistent in reality. This holds for the number densities, that is, the measure of particles per volume, for the microphysical properties like size distribution, refractive index and shape, and for the tallness dissemination [11,12]. In addition, must of the

time the real properties are not known. Hence, it is difficult to demonstrate aerosols and clouds exhaustively. It is important to reduce the changeability of normally happening aerosols and clouds to ordinary cases, yet without disregarding potential changes in the particle's microphysical properties.

Atmospheric mineral dust particles can affect chemical, microphysical, and the visibility of the atmosphere which makes them important when considering both natural and anthropogenic climate effects [13]. Mineral dust absorbs and scatter radiation while on the other hand they act as cloud condensation nuclei (CCN) and ice nuclei (IN) leading to cloud formation and growth as well as influencing albedo, persistence, and other cloud properties [12,13]. The aerosol particles uptake moisture when the relative humidity increases, as such are more soaked with water from the surrounding humid air and swell [16]. As the particle size increases the visibility also reduced. Hence, quantitatively, the variation of the particle size distribution of aerosol particles with relative humidity has to be taken into account [17].

In this work, the extinction coefficients, volume mix ratios, dry mode radii and wet mode radii of desert aerosols were extracted from OPAC (4.0) at the spectral wavelength of 0.4 to 0.8μm, and at relative humidities of 00, 50, 70, 80, 90, 95, 98 and 99%. The four components of the desert aerosols, (WASO, MINN, MIAN MICN) was varied. The parameters were analyzed using excel, SPSS, Origin and some standard formulae to determine the effective hygroscopic growth, humidification factor, visibility enhancement parameter, visibility, the mean exponent of aerosol growth curve and the mean exponent of aerosol size distribution.

2. THEORETICAL FRAMEWORK

An objective measure of visibility is the standard visual range or meteorological range [18].

$$Vis(\lambda) = \frac{3.912}{\sigma_{ext}(\lambda)} \quad (1)$$

Meteorological range refers to the visual range of a black object seen against its surrounding [19]. The visual extinction coefficient $\sigma_{ext}(\lambda)$ is the measure of light scattering and absorbing properties of the atmosphere along the line of sight [12]. To determine the visibility using the extracted extinction coefficient, the variation of the extinction coefficient with wavelength was determined using the inverse power law of extinction coefficient as;

$$\sigma_{ext}(\lambda) = \beta\lambda^{-\alpha} \quad (2)$$

where α and β are known as Angstrom parameters [10]. The index α is the wavelength exponent or Angstrom coefficient and β is the turbidity coefficient representing the number of aerosols present in the atmosphere in the vertical direction or the total aerosol loading in the atmosphere [19, 20].

Substituting equation (2) into (1), the following equation is obtained which is the variation of the visibility with wavelength.

$$Vis(\lambda) = \frac{3.912}{\beta}\lambda^{\alpha} \quad (3)$$

Equation (3) can also be written as

$$ln\left(\frac{Vis_{\lambda}}{3.912}\right) = -ln(\beta) + \alpha\, ln(\lambda) \quad (4)$$

To obtain α (slope) and β (intercept) a regression analysis was performed using an expression derived from the Kaufman (1993) representation of the equation [22].

However, the Angstrom exponent itself varies with wavelength, and a more precise empirical relationship between visibility and wavelength is obtained with a 2nd-order polynomial [10,23-26]

$$ln\left(\frac{Vis_{\lambda}}{3.912}\right) = -ln(\beta) + \alpha_1 ln(\lambda) + \alpha_2\left(ln(\lambda)\right)^2 \quad (5)$$

Here, the coefficient α_2 accounts for a "curvature" often observed in the sun photometry measurements. Some authors have noted that the curvature is also an indicator of the aerosol particle size, with negative curvature indicating aerosol size distributions dominated by the fine mode and positive curvature indicating size distributions with a significant coarse mode contribution [26–29].

Now, to determine the relationship between visibility and relative humidity, enhancement parameter is defined as [17].

$$f(RH,\lambda) = \frac{Vis(RH,\lambda)}{Vis(RH=0,\lambda)} = \left[\frac{1-(RH)}{1-(RH=0)}\right]^{-\gamma} \quad (6)$$

Now taking the natural log of both side we have

$$ln\left(\frac{Vis(RH,\lambda)}{Vis(0,\lambda)}\right) = -\gamma ln(1-RH) \quad (7)$$

Also, γ is given as [5]

$$\gamma = \frac{(v-1)}{\mu} \quad (8)$$

where γ is the humidification factor representing the dependence of visibility on RH, while other terms retain their usual meaning as previously defined. The γ arises from the change in the particle size and refractive indices upon humidification [10,30]. The advantage of γ is that, it describes the hygroscopic behavior of visibility in a linear relationship over a broad range of values of RH, and also implies that particles are deliquesced [31], the γ parameter is dimensionless, and it increases with increase in particle water uptake [9].

Junge have demonstrated the need for using logarithmic range for the interpretation of the mean exponent of the aerosol size distributions [32]. Based on experimental observations, he proposed a power law size distribution function of the form;

$$\frac{dn(r)}{d(logr)} = Cr^{-v} \quad (9)$$

where dn(r) is the number of particles with radii between r and r+dr, C is constant depending on the number of particles in one cubic centimeter and the exponent v determines the mean exponent of aerosol size distribution. As v values increase the number of smaller particles increases compared to larger particles [24].

Now, the hygroscopic growth g(*RH*) experienced by a single aerosol particle according to [17] is given by

$$g(RH) = \frac{r(RH)}{r(RH=0)} \quad (10)$$

where *r(RH)* is the radius at RH% and *r(RH=o)* is the radius at 0%RH.

Now, the effective hygroscopic growth of the four components of the aerosols is given as:

$$g_{eff}(RH) = \left(\sum_i x_i g_i^3(RH)\right)^{\frac{1}{3}} \quad (11)$$

where the summation is performed over all compounds present in the particles and x_i represents the respective volume fraction of single aerosol particle concentration and g_i is the hygroscopic growth of the i^{th} aerosol particles using the Zdanovskii-Stokes-Robinson relation [33], and *i*= 1,2,3,4.

Now, expressing the effective hygroscopic growth in terms of relative humidity we have:

$$g_{eff}(RH) = \left[\frac{1-(RH)}{1-(RH=0)}\right]^{-\frac{1}{\mu}} \quad (12)$$

where μ is defined as the mean exponent of the aerosol growth curve constant as defined in equation (8). Equation (12) can also be written as:

$$\ln\left(g_{eff}(RH)\right) = -\frac{1}{\mu}\ln(1-RH) \quad (13)$$

Now, expressing v (the mean exponent of the aerosol size distribution) in terms of μ (the mean exponent of aerosol growth curve) and γ (the humidification factor) using equations (8) and (12) we have:

$$v = \gamma\mu + 1 \quad (14)$$

3. METHODS

3.1 The OPAC Software Package

The OPAC programming software comprises of two sections, the initial segment is a dataset of microphysical properties and the subsequent optical properties of cloud and aerosols components at various wavelengths and for different relative humidity conditions [18,33]. The other part is a FORTRAN program that permits the user to separate information from this dataset, to compute extra optical properties, and to ascertain optical properties of the mixtures of the stored cloud and aerosols components [18,33]. The dataset gives the microphysical and optical properties for six kinds of water clouds, three ice mists, and 10 aerosols components. the data is accessible at 61 wavelengths in the range of 0.25 and 40 μm for aerosols and clouds, and at 67 wavelengths in the range of 0.28 and 40 μm for ice clouds. The information is given for each case for 1 molecule cm^{-3}which portrays the compelling properties of the combination of all particles in the size distribution. For functional use, the values must be multiplied by the total number density. On account of those aerosols components that can take up water, data for eight values of relative humidities (0%, 50%, 70%, 80%, 90%, 95%, 98%, 99%) are given [18,33]. The information is stored as ASCII files, one record for each cloud or aerosols component and for each relative humidities. The computer code executes two tasks. First, single cloud or aerosols segments can be chosen, and all or a portion of their optical properties can be

extracted or determined from the dataset. Second, it is feasible to choose one of those combinations of the aerosol's components, which are proposed as default values in OPAC, or to characterize an extra mixture and to obtain its optical properties [18,33]. Height placement of aerosols particles is given but may likewise be changed with information given by the user. For versatility, the program is disseminated as FORTRAN source code. All mandatory input to the program must be entered as an ASCII text document [18,33].

3.2 OPAC Operation and Data Generation

To operate OPAC the following steps are followed:

a. the first step is to choose the desired mixture of aerosols or cloud components.
b. the second step deals with choosing the height profile if you are not using the default mixture (i.e here is where you introduce the new profiles).
c. The third step is where you choose the wavelengths for which you want calculate the optical parameters from the already stored data base.
d. The fourth step deals with choosing the relative humidities range for which the calculations of the selected optical parameters should be made.
e. The fifth step is where you choose the optical parameters.
f. The sixth step is where you compile, build and execute the above selection.
g. The seventh step is where you get the calculated optical properties of clouds or aerosols from the output file.
h. The data extracted from OPAC was then imported into excel sheet.

3.3 Data Analysis

This section shows the steps taken in analyzing the data

a. the angstrom exponent/parameter a and the turbidity coefficient b were evaluated using equation (4) which is derived from equations (1), (2) and (3)
b. the curvature a_2 were calculated using equation (5)
c. the humidification factor g was evaluated using equation (7)
d. equation (13) was used to evaluate the mean exponent of aerosols growth curve m.
e. and equation (14) was used to evaluate the mean exponent of aerosols size distribution μ.

3.4 The Model's Components of the Compositions of the Desert Aerosols

Tables 1a-1d shows the models components of the compositions of the desert aerosols used to determine the extinction coefficients of the mixture.

Table 1. The microphysical properties used in simulation

	waso	minn	mian	micn
Minimumradius,[μm]	0.005	0.005	0.005	0.005
Maximumradius,[μm]	20	20	20	60
sigma:	2.24	1.95	2	2.15
Rmod(wet),[μm]	0.0212	0.07	0.39	1.9
Rmod(dry),[μm]	0.0212	0.07	0.39	1.9

Table1a. The models used in the simulations of the desert aerosols (WASO)

	Model1	Model2	Model3	Model4	Model5
Comp	**No. Den. (cm^{-3})**	**No. Den. (cm^{-3})**	**No. Den. (cm^{-3})**	**No. Den. (cm^{-3})**	**No. Den. (cm^{-3})**
WASO	**2200**	**2400**	**2600**	**2800**	**3000**
MINN	269.5	269.5	269.5	269.5	269.5
MIAN	30.5	30.5	30.5	30.5	30.5
MICN	0.142	0.142	0.142	0.142	0.142

Table 1b. The models used in the simulations of the desert aerosols (MINN)

	Model1	Model2	Model3	Modle4	Model5
Comp	**No. Den. (cm^{-3})**	**No. Den. (cm^{-3})**	**No. Den. (cm^{-3})**	**No. Den. (cm^{-3})**	**No. Den. (cm^{-3})**
WASO	2000	2000	2000	2000	2000
MINN	**289.5**	**309.5**	**329.5**	**349.5**	**369.5**
MIAN	30.5	30.5	30.5	30.5	30.5
MICN	0.142	0.142	0.142	0.142	0.142

Table1c. The models used in the simulations of the desert aerosols (MICN)

	Model1	Model2	Model3	Model4	Model5
Comp	**No. Den. (cm^{-3})**	**No. Den. (cm^{-3})**	**No. Den. (cm^{-3})**	**No. Den. (cm^{-3})**	**No. Den. (cm^{-3})**
WASO	2000	2000	2000	2000	2000
MINN	269.5	269.5	269.5	269.5	269.5
MIAN	**40.5**	**50.5**	**60.5**	**70.5**	**80.5**
MICN	0.142	0.142	0.142	0.142	0.142

Table1d. The models used in the simulations of the desert aerosols (MINN)

	Model1	Model2	Model3	Modle4	Model5
Comp	**No. Den. (cm^{-3})**	**No. Den. (cm^{-3})**	**No. Den. (cm^{-3})**	**No. Den. (cm^{-3})**	**No. Den. (cm^{-3})**
WASO	2000	2000	2000	2000	2000
MINN	269.5	269.5	269.5	269.5	269.5
MIAN	30.5	30.5	30.5	30.5	30.5
MICN	**0.142**	**0.152**	**0.162**	**0.172**	**0.182**

4. RESULTS AND DISCUSSIONS

This section presents the results of the analyzed data extracted from OPAC 4.0 based on the models presented in Tables 1a-1d.

4.1 WASO Component

From Fig. 1, it can be observed that the visibility increased with the increase in wavelength, and decreased with the increase in relative humidity (RH). It can also be observed that the visibility is lower at shorter wavelengths which shows the dominance of coarse mode particles with some traces of fine mode particles. It should also be noted that fine mode particles scatter and absorb more solar radiation than the coarse mode particles [7]. Since from equation (3) the visibility is the inverse of extinction, this implies that the visibility will be lower at shorter wavelengths.

From Table 2, by observing the R^2 values from both the linear and quadratic parts, it can be seen that the data fitted the equation models very well. From the linear part, since α is less than 1, this signifies the dominance of coarse mode particles. The increase in α with RH shows that coarse mode particles are being reduced from the atmosphere more than fine mode particles as a result of the increase in RH due to sedimentation of larger particles. Considering the quadratic part, it can be seen that α_2 is negative from RH of 0 to 98%, and this shows monomodal distribution of coarse mode particles. But at RH of 99% it changed to positive and this indicates bimodal type of distribution with coarse mode particles as dominant and traces of fine mode particles. The fluctuations in the magnitudes of α_2 with RH maybe due to non-linearity relation between particles size distribution of the physically mixed aerosols with RH. The increase in the turbidity coefficient β with RH signifies decrease in visibility with increase in RH.

By observing the values of R^2, it can be said that the data fitted the equation models very well. Equation (6) shows that the visibility enhancement parameter satisfies the inverse power law. It can be seen that the mean exponent of the aerosol size distribution (v) and the humidification factor *g* decrease with the increase in wavelengths which implied increase in particle size distribution. And this showed the

reason why the visibility increases with the increase in wavelength due to the increase in the number of larger particles increase compared to smaller particles and this is due to major coagulation amount caused by the increase in number of fine mode particles and consequently the tiny particles coagulate more than the larger particles as said by [14,31]. It can also be observed that, the average value of v=2, and this characterized the weather conditions to be foggy [32].

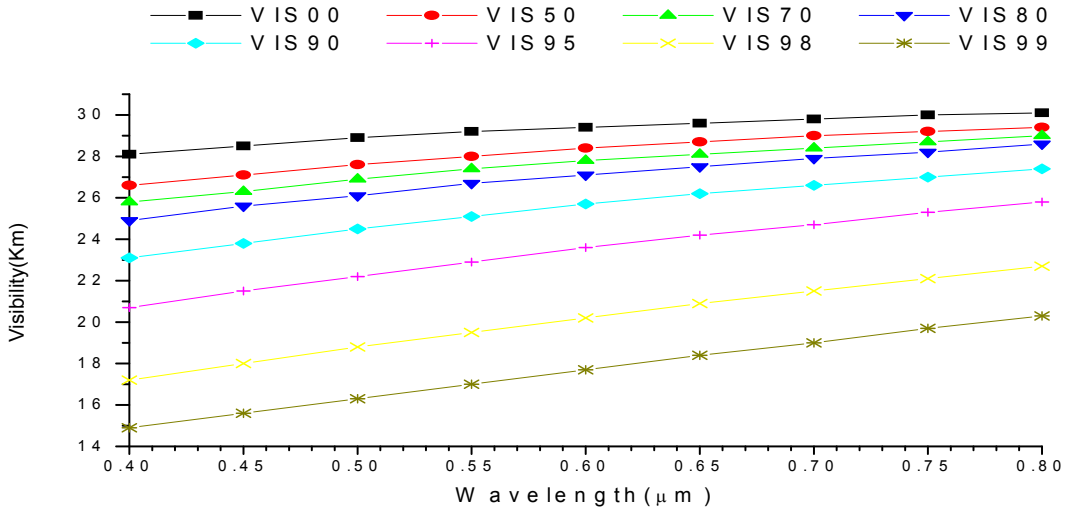

Fig. 1 the plot of visibilities against wavelengths for WASO model 1

Table 2. Results of the regression analysis of equations (4) and (5) for visibility (Model1) using SPSS

	Linear			Quadratic			
RH	**R^2**	**α**	**β**	**R^2**	**α_1**	**α_2**	**β**
0%	0.9756	0.0982	0.1267	0.9866	0.0388	-0.0527	0.1285
50%	0.9968	0.1421	0.1285	0.9970	0.1295	-0.0111	0.1289
70%	0.9892	0.1665	0.1300	0.9962	0.0870	-0.0706	0.1325
80%	0.9947	0.1971	0.1306	0.9966	0.1477	-0.0438	0.1322
90%	0.9963	0.2536	0.1343	0.9977	0.1983	-0.0490	0.1360
95%	0.9977	0.3060	0.1422	0.9985	0.2586	-0.0420	0.1438
98%	0.9990	0.3985	0.1578	0.9990	0.3950	-0.0031	0.1579
99%	0.9978	0.4474	0.1752	0.9991	0.5406	0.0827	0.1714

Table 3. The result of the analysis of equations (7), (13) and (14) using SPSS

	μ	**12.00149**	
λ(μm)	**R^2**	**γ**	**v**
0.55	0.953877	0.096868	2.16256
0.65	0.944524	0.084055	2.008785
0.75	0.936226	0.072915	1.875089

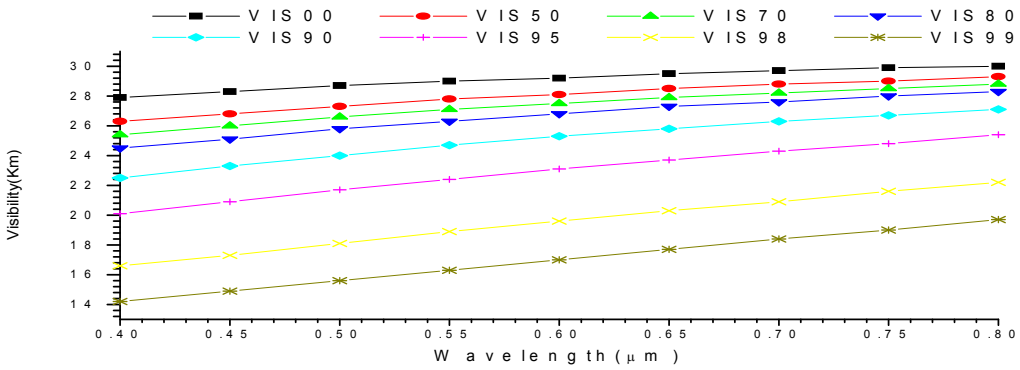

Fig. 2. plot of visibility against wavelength for WASO model 2

From Fig. 2, it can be observed that the visibility increases with the increase in wavelength, and decreases with the increase in relative humidity (RH). It can also be observed that the visibility is lower at shorter wavelength and this can be attributed to the fact that fine mode particles scatter and absorb more solar radiation than the coarse mode particles [7]. Since from equation (3) the visibility is the inverse of extinction, this implies that the visibility will be lower at shorter wavelengths. More so, the rate of increase in visibility with RHs is more pronounced as from 80-99% RHs. It should be noted that only the plots for models 1 and 2 are presented in this paper because they followed the same pattern and same mode of variations for the rest of the models.

From Table 4, observing the values of R^2, it can be said that the data fitted the equation models very well. equation (6) shows that the visibility enhancement parameter satisfies the inverse power law. It can be seen that the mean exponent of the aerosol size distribution (v) and the humidification factor *g* decrease with the increase in wavelengths which implied increase in particle size distribution. And this showed the reason why the visibility increases with the increase in wavelength due to the increase in the number of larger particles increase compared to smaller particles and this is due to major coagulation amount caused by the increase in number of fine mode particles and consequently the tiny particles coagulate more than the larger particles as said by [14,31]. It can also be observed that, the average value of v=2, and this characterized the weather conditions to be foggy [32].

Table 4. The result of the analysis of equations (7) and (13) and (14) using SPSS

	μ	**11.51901**	
λ(μm)	**R^2**	γ	v
0.55	0.955467	0.103468	2.191849
0.65	0.946300	0.090044	2.037218
0.75	0.938456	0.078479	1.904001

Table 5. Results of the regression analysis of equations (4) and (5) for visibility (Model3) using SPSS

	Linear			**Quadratic**			
RH	**R^2**	**α**	**β**	**R^2**	**α_1**	**α_2**	**β**
0%	0.9843	0.1134	0.126802	0.9882	0.0724	-0.0364	0.128042
50%	0.9935	0.1760	0.128343	0.9972	0.1151	-0.0540	0.130211
70%	0.9961	0.2011	0.130197	0.9983	0.1469	-0.0481	0.131883
80%	0.9963	0.2259	0.131952	0.9966	0.2021	-0.0212	0.132702
90%	0.9983	0.2880	0.136142	0.9984	0.2698	-0.0161	0.136729
95%	0.9994	0.3500	0.145064	0.9994	0.3428	-0.0064	0.145313
98%	0.9998	0.4489	0.163625	0.9998	0.4517	0.0024	0.163518
99%	0.9969	0.4899	0.185164	0.9986	0.6041	0.1013	0.180212

From Table 5, by observing the R^2 values from both the linear and quadratic part, it can be seen that the data fitted the equation models very well. From the linear part, α is less than 1, this signifies the dominance of coarse mode particles. The increase in α with RH signifies the reduction in the concentration of the coarse mode particles as they become very heavy as a result of the increase in RH due to sedimentation of larger particles. The negative sign of α_2 from 0 to 95% RH signifies that it is monomodal distribution of coarse mode particles. And from 98 to 99% RHs, a_2 become positive. This signifies the bimodal distribution of coarse mode particles with traces of fine mode particles. The fluctuations in the magnitudes of α_2 show the non-linearity relation between particles size distribution, the physically mixed aerosols with RH. The increase in turbidity coefficient β with RH signifies decrease in visibility with increase in RH. It should also be noted that only the results of the analysis of models 1 and 2 are presented here because they followed the mode of variations all through the rest of the studied models.

From Table 6, observing the values of R^2, it can be said that the data fitted the equation models very well. Equation (6) shows that the visibility enhancement parameter satisfies the inverse power law. It can be seen that the mean exponent of the aerosol size distribution (v) and the humidification factor *g* decrease with the increase in wavelengths which implied increase in particle size distribution. And this showed the reason why the visibility increases with the increase in wavelength due to the increase in the number of larger particles increase compared to smaller particles and this is due to major coagulation amount caused by the increase in number of fine mode particles and consequently the tiny particles coagulate more than the larger particles as said by [14,31]. It can also be observed that, the average value of v=2, and this characterized the weather conditions to be foggy [32].

From Table 8, observing the values of R^2, it can be said that the data fitted the equation models very well. Equation (6) shows that the visibility enhancement parameter satisfies the inverse power law with. It can be seen that the mean exponent of the aerosol size distribution (v) and the humidification factor *g* decrease with the increase in wavelengths which implied increase in particle size distribution. And this showed the reason why the visibility increases with the increase in wavelength due to the increase in the number of larger particles increase compared to smaller particles and this is due to major coagulation amount caused by the increase in number of fine mode particles and consequently the tiny particles coagulate more than the larger particles as said by [14,31]. It can also be noted from the average value of v=2, and this shows that the average atmospheric condition of the area is foggy [32].

Table 6. The result of the analysis of equations (7) and (13) and (14) using SPSS

	μ	**11.10396**	
λ(μm)	**R^2**	γ	v
0.55	0.956928	0.109826	2.219503
0.65	0.948234	0.095862	2.064447
0.75	0.939626	0.08365	1.928846

Table 7. The result of the analysis of equations (7) and (13) and (14) using SPSS

	μ	**10.7446**	
λ(μm)	**R^2**	γ	v
0.55	0.959096	0.116186	2.248372
0.65	0.949607	0.101443	2.089965
0.75	0.940817	0.088632	1.952315

Table 9. The result of the analysis of equations (7) and (13) and (14) using SPSS

	μ	**10.4272**	
λ(μm)	**R^2**	γ	v
0.55	0.960362	0.122097	2.27313
0.65	0.951008	0.106912	2.114793
0.75	0.942173	0.09347	1.974631

From Table 9, observing the values of R^2, it can be said that the data fitted the equation models very well. Equation (6) shows that the visibility enhancement parameter satisfies the inverse power law. It can be seen that the mean exponent of the aerosol size distribution (v) and the humidification factor g decrease with the increase in wavelength which implied increase in particle size distribution. And this showed the reason why the visibility increases with the increase in wavelength due to the increase in the number of larger particles increase compared to smaller particles and this is due to major coagulation amount caused by the increase in number of fine mode particles and consequently the tiny particles coagulate more than the larger particles as said by [14,31]. It can also be observed that, the average value of v=2, and this characterized the weather conditions to be foggy [32].

From Fig. 3 it can be seen that the angstrom exponent a increased with the increase in relative humidity as shown in Tables 2 and 5 respectively. It can also be seen that the variation in the magnitude of the angstrom exponent a follows the same pattern all for WASO all through the 5 models.

3.2 MINN Component

From Fig. 4, it can be observed that the visibility increases with the increase in wavelength, and decreases with the increase in relative humidity (RH). It can also be observed that the visibility is lower at shorter wavelengths with maximum and minimum values of 23.4km and 13.9km respectively. This shows the dominance of coarse mode particles with some traces of fine mode particles. It should also be noted that fine mode particles scatter and absorb more solar radiation than the coarse mode particles [30]. Since from equation (3) the visibility is the inverse of extinction, this implies that the visibility will be lower at shorter wavelengths. The change in visibility is more pronounced from 90%RH to 99%RH.

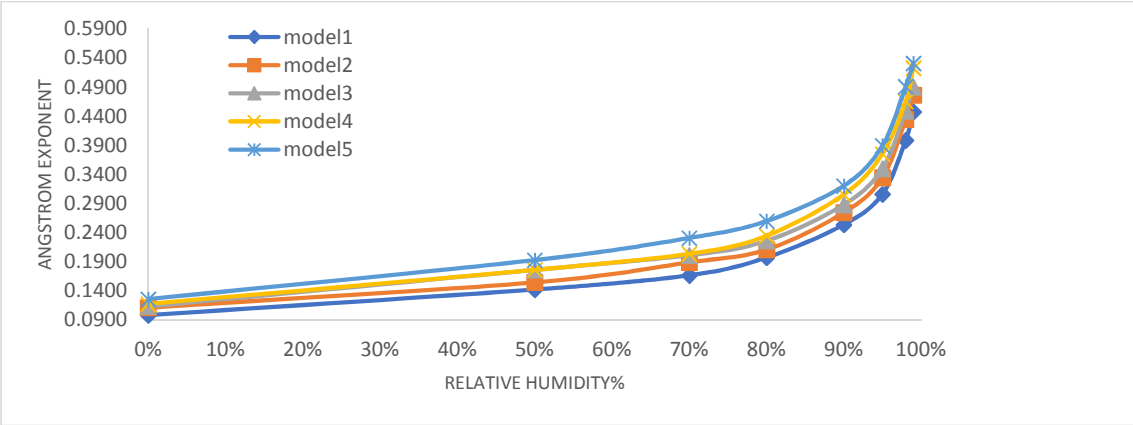

Fig. 3. The plot of angstrom exponent vs relative humidity

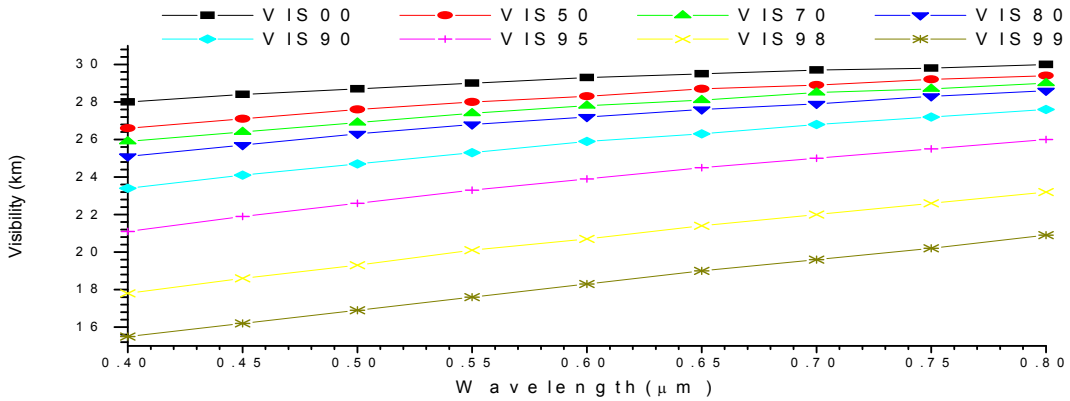

Fig. 4. plot of visibility against wavelengths for minn model 1

Table 10. Results of the regression analysis of equations (4) and (5) for visibility (Model1) using SPSS

	Linear			Quadratic			
RH	**R^2**	**α**	**β**	**R^2**	**α_1**	**α_2**	**β**
0%	0.992800	0.102978	0.127087	0.992868	0.107839	0.004311	0.126941
50%	0.996747	0.142122	0.128528	0.996998	0.129242	-0.01142	0.128922
70%	0.992636	0.156605	0.130402	0.997725	0.092623	-0.05674	0.132397
80%	0.997639	0.192607	0.130643	0.997679	0.185692	-0.00613	0.130857
90%	0.996251	0.234090	0.134475	0.997424	0.188254	-0.04065	0.135946
95%	0.996276	0.299927	0.140320	0.996549	0.271618	-0.02511	0.141266
98%	0.998768	0.376534	0.155441	0.999064	0.413540	0.032819	0.154082
99%	0.998109	0.424610	0.171760	0.998910	0.493203	0.060832	0.168987

Table 11. The result of the analysis of equations (7) and (15) using SPSS

	μ	**12.58748**	
λ(μm)	**R^2**	γ	v
0.55	0.952058	0.089219	2.123043
0.65	0.942307	0.077194	1.971678
0.75	0.934438	0.066949	1.842719

From Table 10, the R^2 values from both linear and quadratic parts shows that the data fitted the equation model very well. From the linear part, since α is less than 1, it signifies the dominance of coarse mode particles, but the magnitudes of α shows that there are some traces of fine mode particles. the increase in α with increase in RH show that coarse mode particles are being removed from the atmosphere more than fine mode particles due to sedimentation of larger particles. From the quadratic part, it can be seen that α_2 is positive at 00%, 98% and 99%RH respectively which shows its bimodal distribution of coarse mode particles. It can also be seen that from 50 to 95% RH it is negative which shows monomodal type of distribution of coarse mode particles. the increase in turbidity coefficient β with RH also signifies that the particles uptake water and swell, which then lead to the decrease in visibility.

Observing the values of R^2 from Table 11, it can be said that the data fitted the equation models very well. Equation (6) shows that the visibility enhancement parameter satisfies the inverse power law. It can be seen that the mean exponent of the aerosol size distribution (v) and the humidification factor *g* decrease with the increase in wavelengths which implied increase in particle size distribution. And this showed the reason why the visibility increases with the increase in wavelength due to the increase in the number of larger particles increase compared to smaller particles and this is due to major coagulation amount caused by the increase in number of fine mode particles and consequently the tiny particles coagulate more than the larger particles as said by [14,31]. It can also be noted that the average value of v=2, this characterized the atmospheric condition of the area to be foggy [32].

It can be seen from Fig. 5 that the visibility increased with the decreased in RH and increased with increase in wavelength and this signifies the dominance of coarse mode particles with some traces of fine mode particles. It can also be observed that the visibility is lower at shorter wavelengths because fine mode particles are more active at shorter wavelength and they tend to scatter more light than coarse mode particles. It should also be noted here that only the plots of models 1 and 2 are presented here because they followed the same pattern and same mode of variations with the rest of the models.

From Table 12, observing the R^2 values from both linear and quadratic parts, it can be seen that the data fitted the equation model very well. From the linear part, it can be seen that α is less than 1, which signifies the dominance of coarse mode particles over fine mode particles. The increase in the magnitude of α with RH signifies that coarse mode particles are removed from the atmosphere more than fine mode particles as a result of sedimentation of the larger particles. From the quadratic part, it can be seen that α_2 is positive at 00, 98 and 99%RH respectively, which shows its bimodal type of distribution. It can also be seen that it is negative from 50 to 95% RH which signifies monomodal type of

distribution. The fluctuations of the magnitudes of α_2 with RH show the non-linearity relation between particles size distribution, the physically mixed aerosols with RH. theincrease in turbidity coefficient β with RH also signifies the particles swelled up due to water uptake and cause the decrease in visibility.

From Table 13, observing the values of R^2, it can be said that the data fitted the equation models very well. Equation (6) shows that the visibility enhancement parameter satisfies the inverse power law. It can be seen that the mean exponent of the aerosol size distribution (v) and the humidification factor g decrease with the increase in wavelengths which implied increase in particle size distribution. And this showed the reason why the visibility increases with the increase in wavelength due to the increase in the number of larger particles increase compared to smaller particles and this is due to major coagulation amount caused by the increase in number of fine mode particles and consequently the tiny particles coagulate more than the larger particles as said by [14,31]. It can also be observed that, the average value of v=2, and this characterized the weather conditions to be foggy [32].

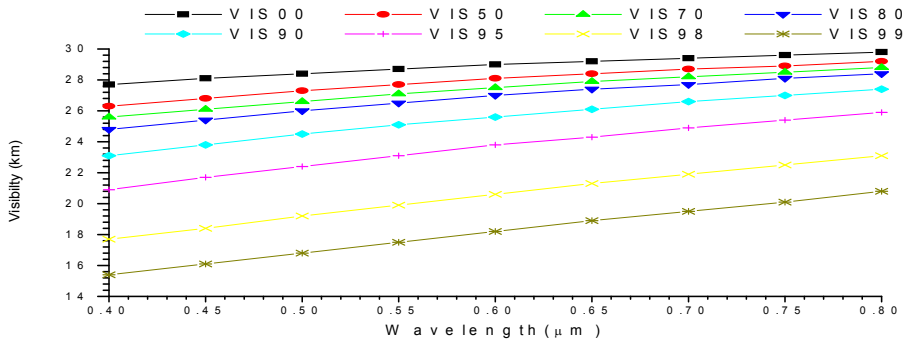

Fig. 5. Plot of visibility against wavelengths for minn model 2

Table 12. Results of the regression analysis of equations (4) and (5) for visibility (Model2) using SPSS

	Linear			Quadratic			
RH	**R^2**	**α**	**β**	**R^2**	**α_1**	**α_2**	**β**
0%	0.992855	0.102978	0.128364	0.992868	0.107839	0.004311	0.128216
50%	0.996747	0.142122	0.12982	0.996998	0.129242	-0.01142	0.130217
70%	0.996306	0.173166	0.130116	0.996397	0.163711	-0.00839	0.130408
80%	0.995291	0.194945	0.131644	0.995926	0.166851	-0.02492	0.132525
90%	0.997992	0.245100	0.134729	0.998024	0.237081	-0.00711	0.134986
95%	0.998486	0.305525	0.140993	0.998587	0.288061	-0.01549	0.141578
98%	0.999404	0.380672	0.156308	0.999505	0.402532	0.019387	0.155578
99%	0.998569	0.438166	0.171278	0.999364	0.508693	0.062547	0.168435

Table 13. The result of the analysis of equations (8) and (12) using SPSS

	μ	**12.60414**	
λ(μm)	**R^2**	**γ**	**v**
0.55	0.951854	0.088453	2.114874
0.65	0.943029	0.076800	1.967998
0.75	0.933635	0.066459	1.837659

Table 14. The result of the analysis of equations (8) and (12) using SPSS

	μ	**12.60637**	
λ(μm)	**R^2**	**γ**	**v**
0.55	0.951666	0.087924	2.108402
0.65	0.945881	0.077633	1.97867
0.75	0.929498	0.065735	1.828679

Observing the values of R^2 from Table 14, it can be said that the data fitted the equation models very well. Equation (6) shows that the visibility enhancement parameter satisfies the inverse power law. It can be seen that the mean exponent of the aerosol size distribution (v) and the humidification factor *g* decrease with the increase in wavelengths which implied increase in particle size distribution. And this showed the reason why the visibility increases with the increase in wavelength due to the increase in the number of larger particles increase compared to smaller particles and this is due to major coagulation amount caused by the increase in number of fine mode particles and consequently the tiny particles coagulate more than the larger particles as said by [14,31]. It can also be observed that, the average value of v=2, and this characterized the weather conditions to be foggy [32].

From Table 15, observing the values of R^2, it can be said that the data fitted the equation models very well. Equation (6) shows that the visibility enhancement parameter satisfies the inverse power law. It can be seen that the mean exponent of the aerosol size distribution (v) and the humidification factor γ decrease with the increase in wavelengths which implied increase in particle size distribution. And this showed the reason why the visibility increases with the increase in wavelength due to the increase in the number of larger particles increase compared to smaller particles and this is due to major coagulation amount caused by the increase in number of fine mode particles and consequently the tiny particles coagulate more than the larger particles as said by [14,31]. It can also be noted that the average value of v=2, this characterized the weather condition of the area to be foggy [32].

By observing the values of R^2 from Table 16, it can be said that the data fitted the equation models very well. Equation (6) shows that the visibility enhancement parameter satisfies the inverse power law. It can be seen that the mean exponent of the aerosol size distribution (v) and the humidification factor *g* decrease with the increase in wavelengths which implied increase in particle size distribution. And this showed the reason why the visibility increases with the increase in wavelength due to the increase in the number of larger particles increase compared to smaller particles and this is due to major coagulation amount caused by the increase in number of fine mode particles and consequently the tiny particles coagulate more than the larger particles as said by [14,31]. It can also be observed that, the average value of v=2, and this characterized the weather conditions to be foggy [32].

From Fig.6 it can be seen that the angstrom exponent α increased with the increase in relative humidity. It can also be seen that the variation in the magnitude of the angstrom exponent a follows the same pattern all for WASO all through the 5 models except for model 5 where it deviates at 70% RH due to nonlinear relation between the physically mixed aerosols with RH.

3.3 MIAN Component

From Fig. 7, it can be observed that the visibility increases with the increase in wavelength, and decreases with the increase in relative humidity (RH). It can also be observed that the visibility is lower at shorter wavelengths with maximum and minimum values of 23.4km and 13.9km respectively. This shows the dominance of coarse mode particles with some traces of fine mode particles. It should also be noted that fine mode particles scatter and absorb more solar radiation than the coarse mode particles [31]. Since from equation (3) the visibility is the inverse of extinction, this implies that the visibility will be lower at shorter wavelengths. The change in visibility is more pronounced from 90%RH to 99%RH.

From Table 17, observing the R^2 values from both the linear and quadratic parts, it can be seen that the data fitted the equation models very well. From the linear part, since α (angstrom exponent) is less than 1, this signifies the dominance of coarse mode particles. The increase in α with RH shows that coarse mode particles are being reduced from the atmosphere more than fine mode particles due to major coagulation and sedimentation of the larger particles as a result of the increase in RH. Considering the quadratic part, it can be seen that α_2 is negative from RH of 0 to 95%, and this shows monomodal distribution of coarse mode particles. But from the RH of 98% to 99% it changed to positive and this indicates bimodal type of distribution with coarse mode particles as dominant and traces of fine mode particles. The fluctuations in the magnitudes of α_2 with RH show the non-linearity relation between particles size distribution, the physically mixed aerosols with RH. The increase in turbidity coefficient β with RH signifies decrease in visibility with increase in RH.

From Table 18, observing the values of R^2, it can be said that the data fitted the equation models very well. Equation (6) shows that the visibility enhancement parameter satisfies the inverse power law. It can be seen that the mean exponent of the aerosol size distribution (v) and the humidification factor *g* decrease with the increase in wavelengths which implied increase in particle size distribution. And this showed the reason why the visibility increases with the increase in wavelength due to the increase in the number of larger particles increase compared to smaller particles and this is due to major coagulation amount caused by the increase in number of fine mode particles and consequently the tiny particles coagulate more than the larger particles as said by [14,31]. It can also be observed that, the average value of v=2, and this characterized the weather conditions to be foggy [32].

From Fig. 8, it can be observed that the visibility increases with the increase in wavelength, and decreases with the increase in relative humidity (RH). It can also be observed that the visibility is lower at shorter wavelengths with the maximum and minimum values of 19.9km and 12.8km which shows the dominance of coarse mode particles with some traces of fine mode particles. It should also be noted that fine mode particles scatter and absorb more solar radiation than the coarse mode particles [31]. Since from equation (3) the visibility is the inverse of extinction, this implies that the visibility will be lower at shorter wavelengths. It can also be noted that the variation in the visibility at lower RHs (00-80) and higher wavelengths is very sharp but it is more pronounced at the higher RHs. It should be noted that only the plots of models 1 and 2 are presented here because they followed same pattern in the variation of the visibility.

Table 15. The result of the analysis of equations (8) and (12) using SPSS

	μ	12.63695	
λ(μm)	R^2	γ	v
0.55	0.951105	0.08691	2.098278
0.65	0.941806	0.075499	1.954077
0.75	0.934048	0.065729	1.830614

Table 16. The result of the analysis of equations (8) and (12) using SPSS

	μ	12.65534	
λ(μm)	R^2	γ	v
0.55	0.950909	0.086183	2.090676
0.65	0.942535	0.075125	1.950733
0.75	0.938431	0.065604	1.830241

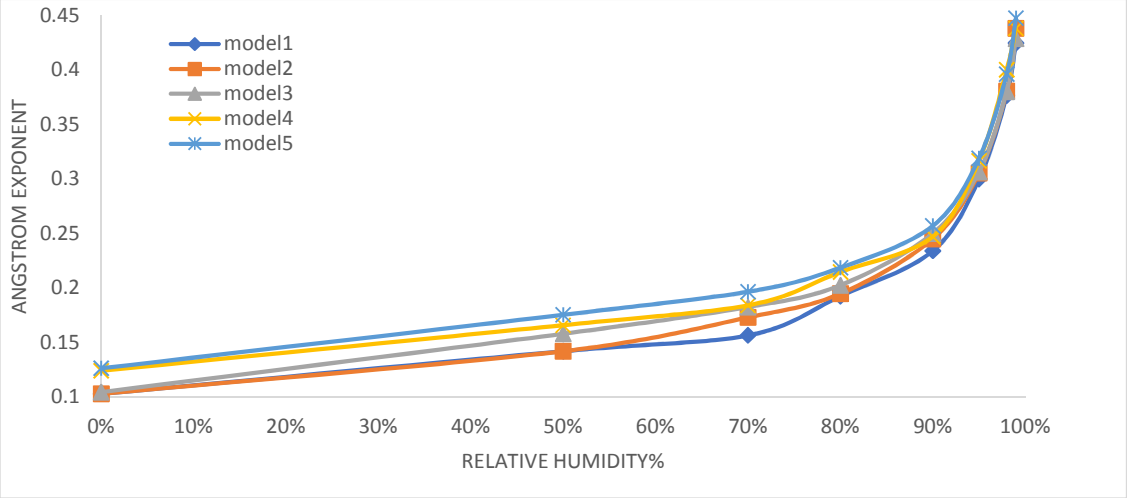

Fig. 6. The plot of angstrom exponent vs relative humidity

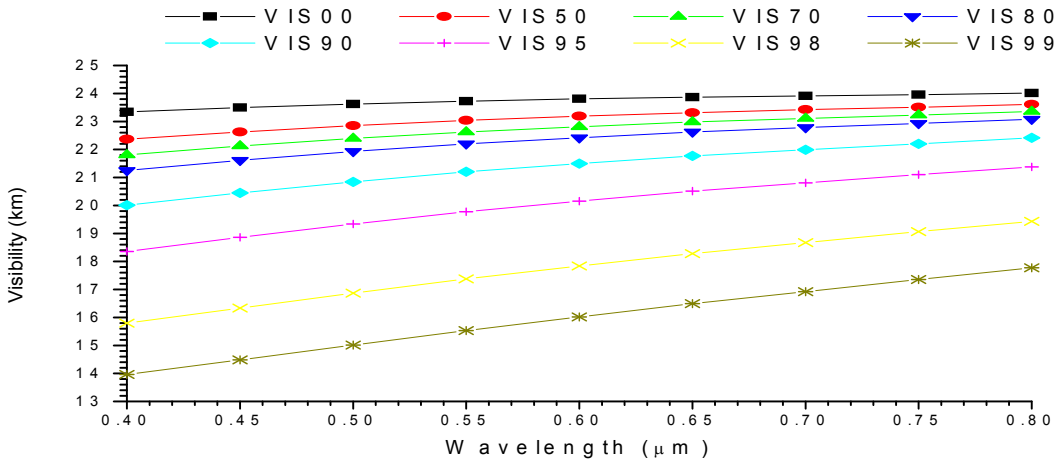

Fig. 7. A graph of visibility against wavelength for Mian model 1

Table 17. Results of the regression analysis of equations (4) and (5) for visibility (Model1) using SPSS

	Linear			Quadratic			
RH	**R^2**	**α**	**β**	**R^2**	**α_1**	**α_2**	**β**
0%	0.853927	0.033923	0.161785	0.907676	0.014641	-0.043067	0.16366
50%	0.963507	0.078151	0.162632	0.966590	0.052932	-0.022367	0.163608
70%	0.979482	0.101566	0.163125	0.981607	0.074572	-0.023940	0.164173
80%	0.964302	0.118551	0.164549	0.989853	0.008444	-0.097649	0.168904
90%	0.996943	0.175504	0.166678	0.997876	0.144870	-0.027168	0.167894
95%	0.997265	0.221988	0.173406	0.997508	0.202203	-0.017547	0.174222
98%	0.999057	0.291584	0.189206	0.999060	0.294414	0.0025132	0.189079
99%	0.998812	0.349628	0.204293	0.998886	0.368064	0.0163587	0.203401

Table 18. The result of the analysis of equations (8) and (12) using SPSS

	μ	**14.09622**	
λ(μm)	**R^2**	γ	v
0.55	0.947681	0.075146	2.059275
0.65	0.938553	0.064349	1.907078
0.75	0.930637	0.055208	1.778224

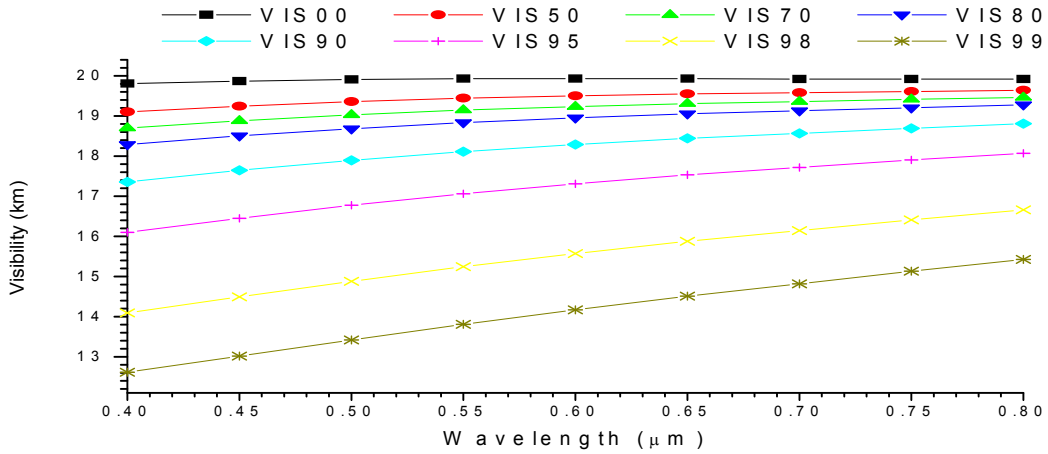

Fig. 8. A graph of visibility against wavelength for mian model 2

Table 19. Results of the regression analysis of equations (4) and (5) for visibility (Model2) using SPSS

	Linear			Quadratic			
RH	R^2	α	β	R^2	α_1	α_2	β
0%	0.366586	0.008555	0.195251	0.718639	0.039281	-0.042424	0.197480
50%	0.853927	0.033923	0.197605	0.907676	0.014640	-0.043067	0.199895
70%	0.911931	0.059966	0.197925	0.982095	0.034949	-0.084168	0.202433
80%	0.983543	0.084078	0.198230	0.987011	0.055593	-0.025263	0.199575
90%	0.988994	0.111533	0.202635	0.993504	0.068558	-0.038113	0.204712
95%	0.989134	0.166572	0.207994	0.996135	0.086610	-0.070916	0.211978
98%	0.998293	0.241554	0.222305	0.998760	0.211749	-0.026433	0.223883
99%	0.999057	0.291584	0.238135	0.999060	0.294414	0.002510	0.237975

Table 20. The result of the analysis of equations (8) and (12) using SPSS

	μ	15.57244	
λ(μm)	R^2	γ	v
0.55	0.945269	0.064713	2.00774
0.65	0.935492	0.054884	1.854678
0.75	0.927849	0.046824	1.729164

By observing the R^2 values from both the linear and quadratic parts of Table 19, it can be seen that the data fitted the equation models very well from the 50%RH to 99%RH but weakly correlated at 00%RH. From the linear part, since α (angstrom exponent) is less than 1, this signifies the dominance of coarse mode particles over fine mode particles. The increase in the magnitudes of α with RH show that coarse mode particles are being removed from the atmosphere more than fine mode particles due to major coagulation and sedimentation of the larger particles. Considering the quadratic part, it can be seen that α_2 is negative from RH of 0 to 98%, and this shows monomodal distribution of coarse mode particles. But at RH of 99% it changed to positive and this indicates bimodal type of distribution with coarse mode particles as dominant and traces of fine mode particles. The fluctuations in the magnitudes of α_2 with RH show the non-linearity relation between particles size distribution, the physically mixed aerosols with RH. The increase in turbidity coefficient β with RH signifies decrease in visibility with increase in RH.

From Table 20, observing the values of R^2, it can be said that the data fitted the equation models very well. Equation (6) shows that the visibility enhancement parameter satisfies the inverse power law. It can be seen that the mean exponent of the aerosol size distribution (v) and the humidification factor *g* decrease with the increase in wavelengths which implied increase in particle size distribution. And this showed the reason why the visibility increases with the increase in wavelength due to the increase in the number of larger particles increase compared to smaller particles and this is due to major coagulation amount caused by the increase in number of fine mode particles and consequently the tiny particles coagulate more than the larger particles as said by [14,31]. It can also be noted that the average value of v=2, this characterized the weather conditions of the area to be foggy [32].

From Table 21, observing the values of R^2, it can be said that the data fitted the equation models very well. Equation (6) shows that the visibility enhancement parameter satisfies the inverse power law. It can be seen that the mean exponent of the aerosol size distribution (v) and the humidification factor *g* decrease with the increase in wavelengths which implied increase in particle size distribution. And this showed the reason why the visibility increases with the increase in wavelength due to the increase in the number of larger particles increase compared to smaller particles and this is due to major coagulation amount caused by the increase in number of fine mode particles and consequently the tiny particles coagulate more than the larger particles as said by [14,31]. It can also be observed that, the average value of v=2, and this characterized the weather conditions to be foggy [32].

From Table 22, observing the values of R^2, it can be said that the data fitted the equation models very well. Equation (6) shows that the visibility enhancement parameter satisfies the inverse

power law. It can be seen that the mean exponent of the aerosol size distribution (v) and the humidification factor *g* decrease with the increase in wavelengths which implied increase in particle size distribution. And this showed the reason why the visibility increases with the increase in wavelength due to the increase in the number of larger particles increase compared to smaller particles and this is due to major coagulation amount caused by the increase in number of fine mode particles and consequently the tiny particles coagulate more than the larger particles as said by [14,31]. It can also be observed that, the average value of v=2, and this characterized the weather conditions to be foggy [32].

From Table 23, observing the values of R^2, it can be said that the data fitted the equation models very well. Equation (6) shows that the visibility enhancement parameter satisfies the inverse power law. It can be seen that the mean exponent of the aerosol size distribution (v) and the humidification factor *g* decrease with the increase in wavelengths which implied increase in particle size distribution. And this showed the reason why the visibility increases with the increase in wavelength due to the increase in the number of larger particles increase compared to smaller particles and this is due to major coagulation amount caused by the increase in number of fine mode particles and consequently the tiny particles coagulate more than the larger particles as said by [14,31]. It can also be observed that, the average value of v=2, and this characterized the weather conditions to be foggy [32].

Table 21. The result of the analysis of equations (8) and (12) using SPSS

	μ	17.02359	
λ(μm)	R^2	γ	v
0.55	0.942339	0.056689	1.965051
0.65	0.934143	0.047976	1.816724
0.75	0.92571	0.040599	1.691141

Table 22. The result of the analysis of equations (8) and (12) using SPSS

	μ	18.4427	
λ(μm)	R^2	γ	v
0.55	0.941089	0.050582	1.932869
0.65	0.93228	0.0425	1.783815
0.75	0.92415	0.035938	1.662794

Table 23. The result of the analysis of equations (8) and (12) using SPSS

	μ	19.84442	
λ(μm)	R^2	γ	v
0.55	0.938951	0.045545	1.903814
0.65	0.930398	0.038161	1.757283
0.75	0.922781	0.032141	1.637819

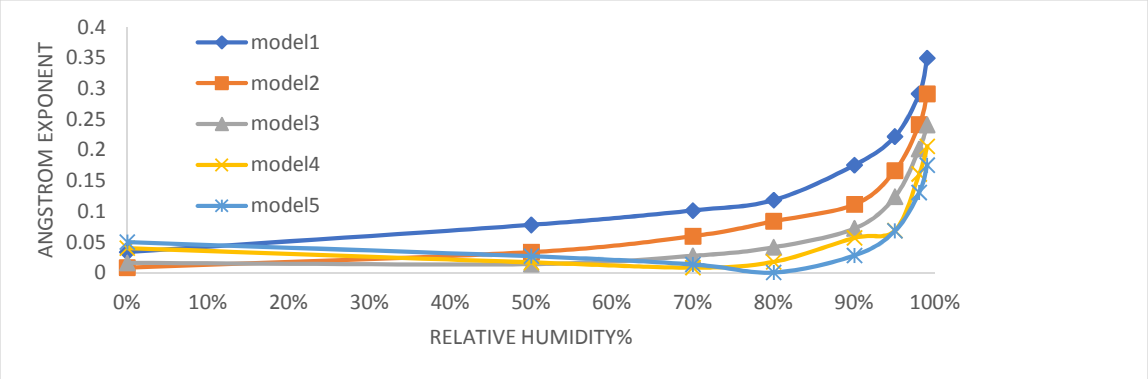

Fig. 9. The plot of angstrom exponent vs relative humidity

From Fig. 9, it can be seen that the angstrom exponent a increased with the increase in relative humidity all through the models except for models 4 and 5 and this might be due to nonlinear relationship between the physically mixed aerosol with RH and with the particles concentration. It can also be seen that the variation in the magnitude of the angstrom exponent a follows the same pattern all through the 5 models for MIAN.

3.4 MICN Component

From fig. 10, it can be observed that the visibility increased with the increase in wavelength, and decreases with the increase in relative humidity (RH). It can also be observed that the visibility is lower at shorter wavelengths with maximum and minimum values of 28.1km and 15.89km respectively. This shows the dominance of coarse mode particles with some traces of fine mode particles. It should also be noted that fine mode particles scatter and absorb more solar radiation than the coarse mode particles [33]. Since from equation (3) the visibility is the inverse of extinction, this implies that the visibility will be lower at shorter wavelengths. The change in visibility is more pronounced from 80%RH to 99%RH and at higher wavelengths.

From Table 24, observing the R^2 values from both the linear and quadratic parts, it can be seen that the data fitted the equation models very well. From the linear part, since α is less than 1, this signifies the dominance of coarse mode particles over fine mode particles. The increase in the magnitudes of α with RH shows that coarse mode particles are being removed from the atmosphere more than fine mode particles due to sedimentation of larger particles. Considering the quadratic part, it can be seen that α_2 is negative from 00% to 98%RH, and this shows monomodal distribution of coarse mode particles with some traces of fine mode particles. It can also be observed from the quadratic part that α_2 is positive at 99%RH, which signifies bimodal type of distribution with coarse mode particles as dominance over fine mode particles. The fluctuations in the magnitudes of α_2 with RH show the non-linearity relation between particles size distribution, the physically mixed aerosols with RH. the increase in turbidity coefficient β with RH also signifies decrease in visibility with increase in RH.

From Table 25, observing the values of R^2, it can be said that the data fitted the equation models very well. Equation (6) shows that the visibility enhancement parameter satisfies the inverse power law. It can be seen that the mean exponent of the aerosol size distribution (v) and the humidification factor *g* decrease with the increase in wavelengths which implied increase in particle size distribution. And this showed the reason why the visibility increases with the increase in wavelength due to the increase in the number of larger particles increase compared to smaller particles and this is due to major coagulation amount caused by the increase in number of fine mode particles and consequently the tiny particles coagulate more than the larger particles as said by [14,31]. It can also be observed that, the average value of v=2, and this characterized the weather conditions to be foggy [32].

From Fig. 11, it can be observed that the visibility increases with the increase in wavelength, and decreases with the increase in relative humidity (RH). It can also be observed that the visibility is lower at shorter wavelengths with maximum and minimum values of 27.9km and 16.89km respectively. This shows the dominance of coarse mode particles with some traces of fine mode particles. It should also be noted that fine mode particles scatter and absorb more solar radiation than the coarse mode particles [33]. Since from equation (3) the visibility is the inverse of extinction, this implies that the visibility will be lower at shorter wavelengths. The change in visibility is more pronounced from 90%RH to 99%RH.

From Table 26, observing the R^2 values from both the linear and quadratic parts, it can be seen that the data fitted the equation models very well. From the linear part, since α (angstrom exponent) is less than 1, this signifies the dominance of coarse mode particles. The increase in α with RH shows that coarse mode particles are being reduced from the atmosphere more than fine mode particles due to sedimentation of larger particles. Considering the quadratic part, it can be seen that α_2 is negative from RH of 0 to 98%, and this shows monomodal distribution of coarse mode particles. But it changed to positive at 99%RH which signifies that it is bimodal type of distribution with coarse mode particles as dominant and traces of fine mode particles. The fluctuations of the magnitudes of α_2 with RH show the non-linearity relation between particles size distribution, the physically mixed aerosols with RH. The increase in turbidity coefficient β with RH signifies decrease in visibility with increase in RH.

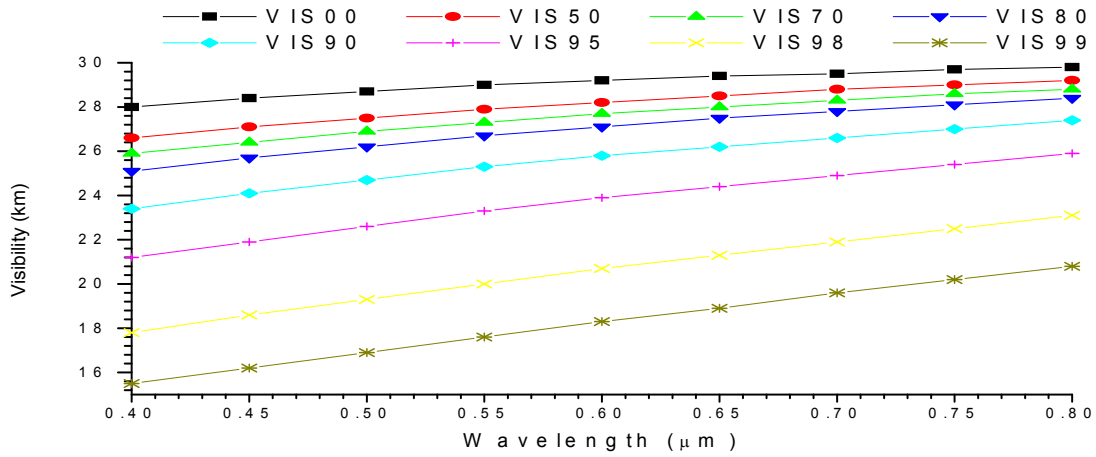

Fig. 10. A graph of visibility against wavelength for micn model 1

Table 24. Results of the regression analysis of equations (4) and (5) for visibility (Model1) using SPSS

	Linear			Quadratic			
RH	**R^2**	**α**	**β**	**R^2**	**α_1**	**α_2**	**β**
0%	0.9852	0.0920	0.1281	0.9891	0.0590	-0.0292	0.1291
50%	0.9834	0.1296	0.1297	0.9928	0.0573	-0.0641	0.1319
70%	0.9965	0.1580	0.1304	0.9978	0.1259	-0.0285	0.1314
80%	0.9935	0.1760	0.1322	0.9972	0.1146	-0.0545	0.1342
90%	0.9953	0.2262	0.1353	0.9963	0.1848	-0.0367	0.1367
95%	0.9991	0.2916	0.1416	0.9991	0.2944	0.0025	0.1415
98%	0.9988	0.3655	0.1567	0.9988	0.3647	-0.0007	0.1567
99%	0.9976	0.4260	0.1718	0.9993	0.5265	0.0891	0.1678

Table 25. The result of the analysis of equations (7), (13) and (14) using SPSS

	μ	**12.7709**	
λ(μm)	**R^2**	**γ**	**v**
0.55	0.952257	0.089078	2.137606
0.65	0.943115	0.077094	1.98456
0.75	0.93441	0.066759	1.852573

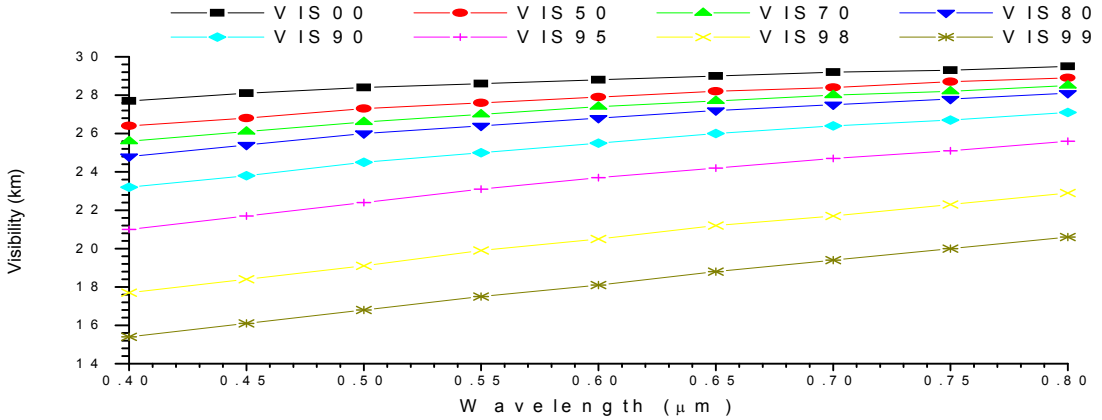

Fig. 11. Plot of visibility against wavelength for micn model 2

Table 26. Results of the regression analysis of equations (4) and (5) for visibility (Model2) using SPSS

	Linear			Quadratic			
RH	**R^2**	**α**	**β**	**R^2**	**α_1**	**α_2**	**β**
0%	0.983543	0.084078	0.130247	0.987011	0.055593	-0.02526	0.13113
50%	0.984782	0.126974	0.131460	0.987153	0.091422	-0.03153	0.132573
70%	0.996531	0.158017	0.131759	0.997796	0.125891	-0.02849	0.132767
80%	0.993475	0.176046	0.133575	0.997192	0.114604	-0.05449	0.135537
90%	0.995262	0.226201	0.136705	0.996284	0.184835	-0.03669	0.138053
95%	0.998324	0.288038	0.143111	0.998457	0.269081	-0.01681	0.143757
98%	0.998805	0.365523	0.158283	0.998806	0.364712	-0.00072	0.158313
99%	0.999067	0.415137	0.173981	0.999513	0.465208	0.044407	0.171926

Table 27. The result of the analysis of equations (8) and (12) using SPSS

	μ	**12.95236**	
λ(μm)	**R^2**	γ	v
0.55	0.951782	0.088183	2.142178
0.65	0.942524	0.076226	1.987307
0.75	0.934189	0.066063	1.855672

Table 28. the result of the analysis of equations (8) and (12) using SPSS

	μ	**13.13008**	
λ(μm)	**R^2**	γ	v
0.55	0.950996	0.087216	2.145153
0.65	0.94189	0.075413	1.990179
0.75	0.933913	0.065305	1.85746

From Table 27, observing the values of R^2, it can be said that the data fitted the equation models very well. Equation (6) shows that the visibility enhancement parameter satisfies the inverse power law. It can be seen that the mean exponent of the aerosol size distribution (v) and the humidification factor *g* decrease with the increase in wavelengths which implied increase in particle size distribution. And this showed the reason why the visibility increases with the increase in wavelength due to the increase in the number of larger particles increase compared to smaller particles and this is due to major coagulation amount caused by the increase in number of fine mode particles and consequently the tiny particles coagulate more than the larger particles as said by [14,31]. It can also be observed that, the average value of v=2, and this characterized the weather conditions to be foggy [32].

From Table 28, observing the values of R^2, it can be said that the data fitted the equation models very well. Equation (6) shows that the visibility enhancement parameter satisfies the inverse power law. It can be seen that the mean exponent of the aerosol size distribution (v) and the humidification factor g decrease with the increase in wavelengths which implied increase in particle size distribution. And this showed the reason why the visibility increases with the increase in wavelength due to the increase in the number of larger particles increase compared to smaller particles and this is due to major coagulation amount caused by the increase in number of fine mode particles and consequently the tiny particles coagulate more than the larger particles as said by [14,31]. It can also be observed that, the average value of v=2, and this characterized the weather conditions to be foggy [32].

Table 29. The result of the analysis of equations (8) and (12) using SPSS

	μ	**13.30796**	
λ(μm)	**R^2**	γ	v
0.55	0.95143	0.086552	2.151831
0.65	0.941556	0.074656	1.993519
0.75	0.93378	0.064638	1.860276

Table 30. The result of the analysis of equations (8) and (12) using SPSS

	μ	13.48636	
λ(μm)	R^2	γ	v
0.55	0.950969	0.08569	2.155646
0.65	0.942124	0.074044	1.998584
0.75	0.933491	0.063985	1.862925

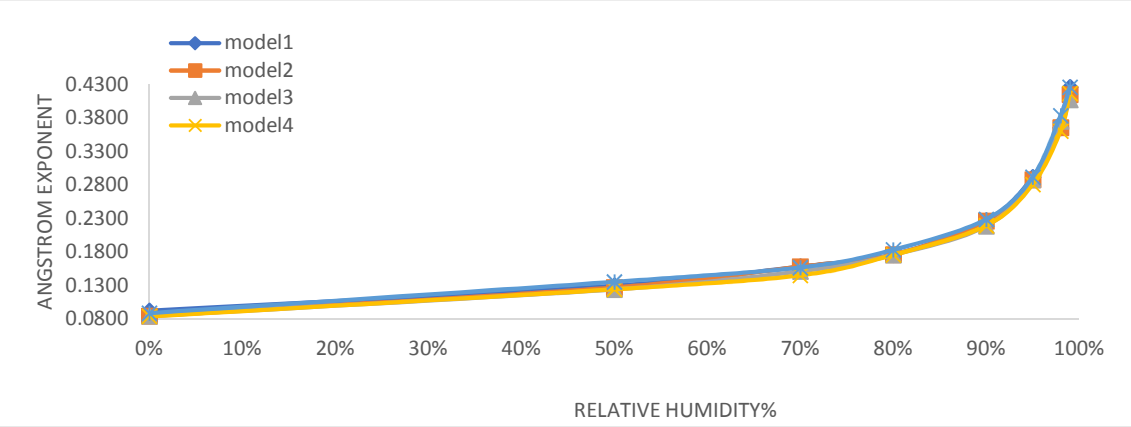

Fig.12. The plot of angstrom exponent vs relative humidity

From Table 29, observing the values of R^2, it can be said that the data fitted the equation models very well. Equation (6) shows that the visibility enhancement parameter satisfies the inverse power law. It can be seen that the mean exponent of the aerosol size distribution (v) and the humidification factor *g* decrease with the increase in wavelengths which implied increase in particle size distribution. And this showed the reason why the visibility increases with the increase in wavelength due to the increase in the number of larger particles increase compared to smaller particles and this is due to major coagulation amount caused by the increase in number of fine mode particles and consequently the tiny particles coagulate more than the larger particles as said by [14,31]. It can also be observed that, the average value of v=2, and this characterized the weather conditions to be foggy [32].

From Table 30, observing the values of R^2, it can be said that the data fitted the equation models very well. Equation (6) shows that the visibility enhancement parameter satisfies the inverse power law. It can be seen that the mean exponent of the aerosol size distribution (v) and the humidification factor *g* decrease with the increase in wavelengths which implied increase in particle size distribution. And this showed the reason why the visibility increases with the increase in wavelength due to the increase in the number of larger particles increase compared to smaller particles and this is due to major coagulation amount caused by the increase in number of fine mode particles and consequently the tiny particles coagulate more than the larger particles as said by [14,31]. It can also be observed that, the average value of v=2, and this characterized the weather conditions to be foggy [32].

From Fig.12, it can be observed that the angstrom exponent a increased with the increase in relative humidity all through the 5 models. It can also be seen that the variation in the magnitude of the angstrom exponent a follows the same pattern all through the 5 models for MICN.

4. SUMMARY

From the models considered (1-5), it was observed that:

I. The (α) angstrom exponent values are less than 1 across the five models and this signifies the dominance of coarse mode particles. Additionally, the increase in RH with the corresponding increase in the concentrations of WASO, MINN, MIAN and MICN caused the magnitude of the angstrom exponent a to fluctuate except

for WASO and this signifies the dominance of coarse mode particles with some traces of fine mode particles.

II. The curvature (α_2) is observed to have both monomodal and bimodal type of distribution at all the RHs, and the magnitude fluctuate for both (WASO, MINN, MIAN and MICN concentrations) across the five models. The fluctuations might be due non-linear relationship between particles size distribution, RH and also with the physically mixed aerosols.

III. It can be observed that the turbidity coefficient β fluctuates with the increase in RH and the concentration of (WASO, MINN, MIAN and MICN) across all the models, this also implies the dominance of coarse mode particles with some traces of fine mode particles.

IV. It should also be noted that the humidification factor (γ) decreased with wavelength all through except for WASO and this might be due to the fact that: WASO are more active at shorter wavelength, at the higher wavelength coarse particles absorbed more water than fine mode particles, fine mode particles are more active shorter wavelength and as we increase the non-hygroscopic particles, we decreased the deliquescence.

V. Based on the results of the analysis of equation (12), it can be seen that the magnitude of μ increased except for WASO and this shows that the effective hygroscopic growth (g_{eff}) also increased except in the case of WASO which decreased with the increase in concentration. The decreased in the magnitude of μ for WASO might be due to the fact that as we increase the non-hygroscopic particles, we decrease the deliquescence.

VI. It should be observed that the mean exponent of aerosol size distribution μ increased with the increase in concentration for WASO and MICN but decreased with the increase in concentration for MINN and MIAN, and this signifies nonlinear relation between the physically mixed aerosols with the size distribution.

VII. The turbidity coefficient (β) also fluctuates with the increase in RH across the models and for all the studied components. this signifies that the particles swelled up as they uptake water and eventually they dropped due major coagulation and sedimentation. This might be due to nonlinear relation between the physically mixed aerosols and their particles size distribution with RH.

VIII. It can also be seen from the work that the values of the mean exponent of aerosols size distribution n for all the components and the studied models are less than 3, this signifies foggy condition for the desert atmosphere.

5. CONCLUSION

The results in this investigation revealed that, the visibility, the visibility decreased with the increase in RH and WASO, MIAN, MINN and MICN (particles concentrations) but decreased with the increase in wavelengths across models and this signifies that larger particle are being removed from the desert atmosphere due major coagulation and sedimentation. The fluctuations in the magnitude of (α) across the models signifies the nonlinear relation between the physically mixed aerosols with RH, and this implies the dominance of coarse mode particles over fine mode particles except for WASO which increased across the models, and this further shows that there is an emergence of larger particles over smaller particles. It should be noted that only the plots and the results of the analysis of models 1 and 2 are presented in this work because they followed same mode variations and patterns all through the remaining models. The fluctuations in the magnitudes of (α_2) as a result of the change in RHs and particle concentrations across the five models also signifies nonlinear relationship between RH and the physically mixed aerosols. It can also be concluded that there is a direct inverse power relation between the humidification factor, the mean exponent of aerosols size distribution with the mean exponent of aerosols growth curve. Further investigation showed that, as the magnitude of μ increased for MIAN, MINN and MICN, the effective hygroscopic growth g_{eff} decreased. For WASO it is also revealed that as the magnitude of μ decreased, the effective hygroscopic growth g_{eff} increased with the increase in particles concentrations and RH. The decreased in the magnitude of μ for WASO might be due to the fact that as we increase the non-hygroscopic particles, we decrease the deliquescence.

COMPETING INTERESTS

Authors have declared that no competing interests exist.

REFERENCES

1. Denjean C, et al. "Size distribution and optical properties of mineral dust aerosols transported in the western Mediterranean," Atmos. Chem. Phys., vol. 16, no. 2, pp. 1081–1104, 2016, doi: 10.5194/acp-16-1081-2016.
2. Srivastava P, Dey S, Kumar A, Singh S, Mishra SK, Tiwari S. "Science of the Total Environment Importance of aerosol non-sphericity in estimating aerosol radiative forcing in Indo-Gangetic Basin," Sci. Total Environ. 2017;599–600:655–662, doi: 10.1016/j.scitotenv.2017.04.239.
3. Griggs DJ, Noguer M. "Climate change 2001: The scientific basis. Contribution of working group I to the third assessment report of the intergovernmental panel on climate change," Weather, 2002;57(8):P 267–269.
DOI: 10.1256/004316502320517344.
4. Carrico CM. "Mixtures of pollution, dust, sea salt, and volcanic aerosol during ACE-Asia: Radiative properties as a function of relative humidity," J. Geophys. Res. 2003;108(D23):8650.
DOI: 10.1029/2003JD003405.
5. Tijjani BI. "The Effect of Soot and Water Soluble on the Hygroscopicity of Urban Aerosols," Adv. Phys. Theor. Appl. , 2013;26(1);52–73. [Online].
Available: www.iiste.org.
6. Ogren JA, Charlson RJ. "Implications for models and measurements of chemical inhomogeneities among cloud droplets," Tellus B, 1992;44(3):208–225.
DOI: 10.1034/j.1600-0889.1992.t01-2-00004.x.
7. Megahed K., "The Impact of Mineral Dust Aerosol Particles on Cloud Formation," 2006.
8. Mishra SK, Tripathi SN, Aggarwal SG, Arola A. "Optical properties of accumulation mode, polluted mineral dust: Effects of particle shape, hematite content and semi-external mixing with carbonaceous species," Tellus, Ser. B Chem. Phys. Meteorol., 2012;64(1).
doi: 10.3402/tellusb.v64i0.18536.
9. Osborne SR, Johnson BT, Haywood JM, Baran AJ, Harrison MAJ, Mc Connell CL. "Physical and optical properties of mineral dust aerosol during the Dust and Biomass-burning Experiment," J. Geophys. Res. Atmos. 2008;113(23):1–14.
DOI: 10.1029/2007JD009551.
10. Tijjani BI, Sha'aibu F, Aliyu A. "The Effect of Relative Humidity on Maritime Tropical Aerosols," Open J. Appl. Sci. 2014;04(06):299–322.
DOI: 10.4236/ojapps.2014.46029.
11. Koepke P, Gasteiger J, Hess M., "Technical Note: Optical properties of desert aerosol with non-spherical mineral particles: Data incorporated to OPAC," Atmos. Chem. Phys. , 2015; 15(10):5947–5956
doi: 10.5194/acp-15-5947-2015.
12. schult IM, Hess P. Koepke, "Optical Properties of Aerosols and Clouds: The Software Package OPAC," 1998; 831–844.
13. Herich H, et al. "Water uptake of clay and desert dust aerosol particles at sub- and supersaturated water vapor conditions," Phys. Chem. Chem. Phys. 2009;11(36):7804–7809.
DOI: 10.1039/b901585j.
14. Sataloff RT, Johns MM, Kost KM, "Climate: The Influence of Aerosols," 1969;8(1):451–456.
15. Camino C, et al. "An empirical equation to estimate mineral dust concentrations from visibility observations in Northern Africa," Aeolian Res., 2018;16:55–68.
DOI: 10.1016/j.aeolia.2014.11.002.
16. Lang R, Xanh NX. "Smoluchowski's theory of coagulation in colloids holds rigorously in the Boltzmann-Grad-limit," Zeitschrift für Wahrscheinlichkeitstheorie und Verwandte Gebiete. 1980;54(3):227–280.
DOI: 10.1007/BF00534345.
17. Kasten F., "Visibility forecast in the phase of pre-condensation," Tellus, 1969 ;21(5):631–635
DOI: 10.3402/tellusa.v21i5.10112.
18. Tsilimigras P. "On the applicability of the Roothaan-Bagus procedure," Chem. Phys. Lett., 1971;11(1):99–100
DOI: 10.1016/0009-2614(71)80541-9.
19. Charlson RJ. "current research," 1969;3(10):913–918.
20. Moorthy KK, Saha A, Prasad BSN, Niranjan, D. Jhurry, and P. S. Pillai, "Aerosol optical depths over peninsular India and adjoining oceans during the INDOEX campaigns: Spatial, temporal, and spectral characteristics," J. Geophys. Res. Atmos. 2001;106(D22):28539–28554
DOI: 10.1029/2001JD900169.
21. Singh S, Nath S, Kohli R, Singh R. "Aerosols over Delhi during pre-monsoon months : Characteristics and effects on

surface radiation forcing," Geophys. Res. Lett. 2005;32(1):4–7.
DOI: 10.1029/2005GL023062.

22. Koschmieder EL. "Symmetric Circulations of Planetary Atmospheres," Adv. Geophys. 1978;20(C):131–181.
DOI: 10.1016/S0065-2687(08)60323-4.
23. M. D. and D. M. B. King, "a method for inferring total ozone content from spectral variation of total optical depth obtained with solar radiometer." 1976;2242–2251.
24. Tijjani BI, Sha'aibu F., Aliyu A., "The Effect of Relative Humidity on Maritime Polluted Aerosols," Open J. Appl. Sci. 2014;04(06):299–322.
DOI: 10.4236/ojapps.2014.46029.
25. O'Neill NT, Dubovik O, Eck TF. "Modified Ångström exponent for the characterization of submicrometer aerosols," Appl. Opt. 2001;40(15):2368
DOI: 10.1364/ao.40.002368.
26. O'Neill NT, Eck TF, Smirnov A, Holben BN, Thulasiraman S. "Spectral discrimination of coarse and fine mode optical depth," J. Geophys. Res. D Atmos., 2003;108(17):1–15,
DOI: 10.1029/2002jd002975.
27. Yoram Kaufman J. "Aerosol Optical Thickness and Atmospheric Path Radiance," Geophys. Res. Lett. 1993;98(2):2677–2692
28. Eck TF, Holben BN, Smirnov A, Slutsker I, Lobert JM, Ramanathan V."Column-integrated aerosol optical properties over the Maidives during the northeast," Geophys. Res. Lett., 2001;106(22):28555–28566.
29. Reid JS, Smirnov A, Neill NTO, Slutsker I, Kinne S. "Wavelength dependence of the optical depth of biomass burning, urban, and desert aerosols," Geophys. Res. 1999;104(1):31333–31349,
30. Eck TF, et al. "Characterization of the optical properties of biomass burning aerosols in Zambia during the 1997 ZIBBEE field campaign," Geophys. Res. 2001;106(4):3425–3448,
31. Quinn PK. et al. "Impact of particulate organic matter on the relative humidity dependence of light scattering: A simplified parameterization," Geophys. Res. Lett. 2005;32(22):1–4,
DOI: 10.1029/2005GL024322.
32. Junge et al., "Chapter 2 Physical and Optical properties of aerosols," Geophys. Res. Lett. 1958; 1(1): L220–247,
33. Sjogren S, Gysel M, Weingartner E, Baltensperger U, Cubison MJ, Coe H. "Hygroscopic growth and water uptake kinetics of two-phase aerosol particles consisting of ammonium sulfate , adipic and humic acid mixtures," Aerosol Sci. 2007;38(1): 157–171.
DOI: 10.1016/j.jaerosci.2006.11.005.

Peer-review history:
The peer review history for this paper can be accessed here:
https://www.sdiarticle4.com/review-history/70740